Advances in Applied Mathematics and Mechanics
Adv. Appl. Math. Mech., Vol. **10**, No. 6, pp. 1418-1439

DOI: 10.4208/aamm.OA-2017-0292
December 2018

Improved Symmetry Property of High Order Weighted Essentially Non-Oscillatory Finite Difference Schemes for Hyperbolic Conservation Laws

Wai Sun Don[1], Peng Li[2], Kwun Ying Wong[3] and Zhen Gao[1,*]

[1] *School of Mathematical Sciences, Ocean University of China, Qingdao 266100, Shandong, China*
[2] *Department of Mathematics and Physics, Shijiazhuang Tiedao University, Shijiazhuang 050043, Hebei, China*
[3] *N. T. Heung Yee Kuk Yuen Long District Secondary School, Hong Kong*

Received 9 November 2017; Accepted (in revised version) 8 February 2018

Abstract. This study aims to investigate the rapid loss of numerical symmetry for problems with symmetrical initial conditions and boundary conditions when solved by the seventh and higher order nonlinear characteristic-wise weighted essentially non-oscillatory (WENO) finite difference schemes. Using the one-dimensional double rarefaction wave problem and the Sedov blast-wave problems, and the two-dimensional Rayleigh-Taylor instability (RTI) problem as examples, we illustrate numerically that the sensitive interaction of the round-off error due to the numerical unstable explicit form of the local lower order smoothness indicators in the nonlinear weights definition, which are often given and used in the literature, and the nonlinearity of the WENO scheme are responsible for the rapid growth of asymmetry of an otherwise symmetric problem. An equivalent but compact and numerical stable compact form of the local lower order smoothness indicators is suggested for delaying the onset of and reducing the magnitude of the symmetry error. The benefits of using the compact form of the local lower order smoothness indicators should also be applicable to non-symmetrical strongly non-linear problems in terms of improved numerical stability, reduced rounding errors and increased computational efficiency.

AMS subject classifications: 65M06, 65N06

Key words: Weighted essentially non-oscillatory, symmetry, smoothness indicator, hyperbolic conservation laws.

1 Introduction

*Corresponding author.
Emails: donwaisun@outlook.com (W. S. Don), weilailp@163.com (P. Li), yingwky@gmail.com (K. Y. Wong), zhengao@ouc.edu.cn (Z. Gao)

Characteristic-wise Weighted Essentially Non-Oscillation (WENO) conservative finite difference schemes are a class of high order/resolution nonlinear schemes for simulating flows with both shock waves and small scale structures that were initially developed in [11] (for details and history of the WENO scheme, see [19] and references therein). The WENO scheme employs a dynamic set of substencils where a nonlinear convex combination of lower order polynomials *adapts* either to a higher degree polynomial approximation at smooth stencils, or to a lower degree polynomial that avoids interpolation of the function across discontinuities at the cell boundary.

The high (fifth and higher) order WENO schemes with the global Lax-Friedrichs flux splitting (GLF) via the Roe-averaged eigensystem have also been applied to the solution of highly unstable fluid flows with a perturbed interface separating two fluids with different densities. One of the well-known examples is the Richtmyer-Meshkov instability (RMI) (see, e.g., [1, 7, 14, 21] and references therein). The interface is accelerated impulsively by a passing shock wave. The interface perturbation grows linearly initially forming a system of bubbles and spikes, and then nonlinearly after the amplitude of the perturbation becomes sufficiently larger. In the meantime, a large amount of vorticity is created and deposited along the interface where the pressure gradient is perpendicular to the density gradient forming vortical rollup in the shape of the mushroom cap. A similar temporal and spatial evolution can also be found in the Rayleigh-Taylors instability (RTI) (see, e.g., [1,15,22,25] and references therein), where a heavy density fluid rests on top of a lighter density fluid. Instead of an impulsive acceleration of the interface by a passing shock, the perturbed interface is accelerated by a constant bulk force, such as the gravity. This phenomenon can often be observed in a lava lamp.

We are motivated by the recent observations about the fact that these highly unstable fluid systems lose the spatial symmetry of an otherwise symmetrical solution under a symmetrical setup and a sinusoidal perturbation on the interface rapidly when solved by the seventh and ninth order WENO schemes. For example, Fig. 1 shows the density of the RTI problem with a sinusoid perturbation and the temporal history of the symmetry error, which measures the L^2 error in the deviation of the symmetry between the left and right half of the density (see Definition 4.1 below), as computed by the ninth order WENO-JS9 scheme at a very high resolution. Even though the density seems to be symmetric about $x=0.125$ in the eyeball norm, the symmetry error $\mathcal{O}(10^{-11})$ is actually much larger than the machine error $\mathcal{O}(10^{-16})$ at the early time and grows fairly large $\mathcal{O}(10^{-4})$ rapidly at the later time.

In this study, we systematically investigate and identify the source(s) of the symmetry error. It is a surprise to find out that the commonly used explicit form of the local lower order smoothness indicators β_k (smoothness indicators) used in the definition of the nonlinear weights ω_k in a substencil S_k for the seventh and ninth order WENO schemes [5] is the source of rounding off errors, and when interact with the nonlinearity of the WENO scheme, can have a strong influence on the symmetry of the solution. For example, the explicit form of β_k given by Balsara et al. [5] is far less accurate and less numerically stable in term of rounding off errors. A loss of four or more significant digits can be devastating

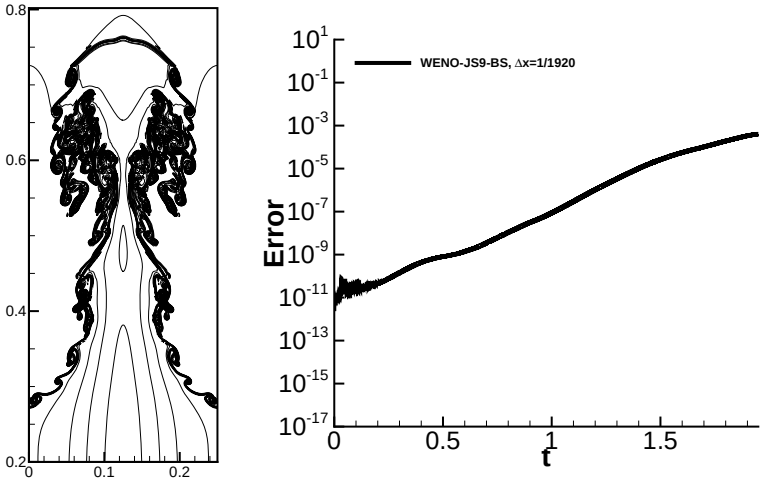

(a) (b)

Figure 1: Two-dimensional Rayleigh-Taylors instability. (a) The density and (b) the symmetry error computed by the WENO-JS9 scheme with $\Delta x = 1/1920$.

to problems which are physically unstable inherently and when solved by a nonlinear shock capturing scheme such as the WENO schemes.

In this work, we would like to emphasize the following two observations:

- By reducing this particular source of numerical errors, one can be confident that the symmetrical solution, when simulated by a high order nonlinear WENO scheme, is not unnecessary overwhelmed by the numerical error prematurely.

- Even though the benefits of using the compact form of β_k is illustrated with problems with symmetrical solutions, the numerical solution of a non-symmetrical strongly non-linear problem can also be benefited in terms of improved numerical stability, reduced rounding off error and increased computational efficiency [3].

This paper is organized as follows. In Section 2, we briefly review the governing equations and the nonlinear WENO finite difference scheme. In Section 3, a brief introduction to the explicit [5] and compact [9] forms of the smoothness indicators β_k used in the definition of the WENO nonlinear weights ω_k. In Section 4, the one-dimensional double rarefaction wave and Sedov blast-wave problems, and the two-dimensional Rayleigh-Taylors instability with symmetrical solution are used as examples to illustrate the rapid loss and improvement of the symmetry when simulated by the seventh and ninth order WENO finite difference schemes with the explicit and compact forms of the smoothness indicators β_k respectively. Concluding remarks are given in Section 5. In Appendix A, one example of the Matlab code for sum of squares via Shur complement is given.

2 WENO finite difference scheme

In this work, we shall consider the hyperbolic conservation laws with the form

$$\mathbf{Q}_t+\nabla\cdot\overrightarrow{\mathbf{F}}=\mathbf{0}, \tag{2.1}$$

in cartesian coordinates. For the two-dimensional case, $\overrightarrow{\mathbf{F}}=(\mathbf{F},\mathbf{G})$ where

$$\mathbf{Q}=(\rho,\rho u,\rho v,E)^T, \tag{2.2a}$$

$$\mathbf{F}=\left(\rho u,\rho u^2+P,\rho uv,(E+P)u\right)^T, \tag{2.2b}$$

$$\mathbf{G}=\left(\rho v,\rho uv,\rho v^2+P,(E+P)v\right)^T, \tag{2.2c}$$

where ρ is density, P is pressure, and $\mathbf{U}=(u,v)$ is the velocity vector. The ideal gas equation of state (EOS) closes the system of equations with

$$P=(\gamma-1)\left(E-\frac{1}{2}\rho\left(u^2+v^2\right)\right), \tag{2.3}$$

where γ is the ratio of specific heats. The source term, if exists, accounts for the effect of the gravity on the fluid in the Rayleigh-Taylors instability (RTI).

To solve the nonlinear system of hyperbolic conservation laws above, we shall use the high order weighted essentially non-oscillatory (WENO) scheme. Below is a brief description of the classical WENO-JS and improved WENO-Z finite difference scheme for solving a nonlinear scalar hyperbolic equation (without the source term) in one dimension. Higher dimensional problems will be handled in a dimensional by dimensional manner. Readers are referred to the literature [19] for discussion on other similar variants of the WENO finite difference schemes.

Consider an equidistant grid defined by the points $x_i=i\Delta x$, $i=0,\cdots,N$, which are cell centers, with cell boundaries $x_{i+\frac{1}{2}}=x_i+\frac{\Delta x}{2}$, where Δx is the uniform grid spacing. The semi-discretized form of (2.1) forms a system of ordinary differential equations (ODE) that will be solved by the third order Runge-Kutta TVD scheme,

$$\frac{dQ_i(t)}{dt}=-\left.\frac{\partial f}{\partial x}\right|_{x=x_i},\quad i=0,\cdots,N, \tag{2.4}$$

where $Q_i(t)$ is a numerical approximation to the cell-averaged value $Q(x_i,t)$.

To form the flux difference across the uniformly spaced cells and to obtain a high-order numerical flux consistent with the hyperbolic conservation laws, a conservative finite difference formulation is required at the cell boundaries. By defining a numerical flux function $h(x)$ implicitly, one has

$$f(x)=\frac{1}{\Delta x}\int_{x-\frac{\Delta x}{2}}^{x+\frac{\Delta x}{2}}h(\xi)d\xi, \tag{2.5}$$

such that the spatial derivative in (2.4) is approximated by a conservative finite difference formula at the cell center x_i,

$$\frac{dQ_i(t)}{dt} = -\frac{1}{\Delta x}\left(h_{i+\frac{1}{2}} - h_{i-\frac{1}{2}}\right), \tag{2.6}$$

where $h_{i\pm\frac{1}{2}} = h(x_{i\pm\frac{1}{2}})$. For a $(2r-1)$ order WENO scheme, $(2r-1)$ order polynomial interpolation to $h_{i\pm\frac{1}{2}}$ are computed using the known cell-averaged values $f_j = f(x_j)$, $j = i-(r-1),\cdots,i+(r-1)$.

The key idea of the WENO methodology is the following polynomial reconstruction procedure. By taking the ($r=3$, $2r-1=5$) order WENO scheme for example, the five-points global stencil $S^5 = (x_{i-2},\cdots,x_{i+2})$ is subdivided into three three-points substencils $\{S_k = (x_{i+k-2},x_{i+k-1},x_{i+k}),\ k=0,1,2\}$. The fifth degree polynomial approximation $\hat{f}_{i\pm\frac{1}{2}} = h_{i\pm\frac{1}{2}} + \mathcal{O}(\Delta x^5)$ is built through the convex combination of three second degree interpolation polynomials $\hat{f}^k(x)$ in substencils S_k at the cell boundaries $x_{i\pm\frac{1}{2}}$,

$$\hat{f}_{i\pm\frac{1}{2}} = \sum_{k=0}^{2} \omega_k^{\pm} \hat{f}^k(x_{i\pm\frac{1}{2}}), \quad \hat{f}^k(x_{i+\frac{1}{2}}) = \sum_{j=0}^{2} c_{kj} f_{i-k+j}, \quad i=0,\cdots,N, \tag{2.7}$$

with Lagrangian interpolation coefficients c_{kj} [11].

- In the classical WENO-JS5 scheme [11], the nonlinear weights ω_k are defined as

$$\omega_k = \frac{\alpha_k}{\sum_{j=0}^{2}\alpha_j}, \quad \alpha_k = \frac{d_k}{(\beta_k+\epsilon)^p}, \quad k=0,1,2.$$

- In the improved WENO-Z5 scheme [6,8], the nonlinear weights ω_k are defined as

$$\omega_k = \frac{\alpha_k}{\sum_{l=0}^{2}\alpha_l}, \quad \alpha_k = d_k\left(1+\left(\frac{\tau_5}{\beta_k+\epsilon}\right)^p\right), \quad k=0,1,2, \tag{2.8}$$

  where $\tau_5 = |\beta_2-\beta_0|$, which has a leading truncation error of order $\mathcal{O}(\Delta x^5)$ in the absence of critical points.

The coefficients $\left\{d_0=\frac{3}{10},\ d_1=\frac{3}{5},\ d_2=\frac{1}{10}\right\}$ are the ideal weights that, when the solution is sufficiently smooth, one has $\{\omega_k \approx d_k,\ k=0,1,2\}$ and the WENO scheme essentially becomes the optimal fifth order central upwind scheme. The sensitivity parameter ϵ is used to avoid the division by zero in the denominator and power parameter p is chosen to increase the difference of scales of distinct weights at the non-smooth stencils of the solution [9,16].

Remark 2.1. An improved WENO-Z scheme has been used extensively and is less dissipative and has higher resolution power than the classical WENO-JS scheme for a larger class of problems. Readers are referred to the literature for the higher order WENO scheme [8,19].

3 Local lower order smoothness indicators β_k

The regularity of the interpolation polynomial approximation $\hat{f}^k(x)$ of the substencil S_k at x_i is measured by the local lower order smoothness indicators,

$$\beta_k=\sum_{l=1}^{r-1}\Delta x^{2l-1}\int_{x_{i-\frac{1}{2}}}^{x_{i+\frac{1}{2}}}\left(\frac{d^l}{dx^l}\hat{f}^k(x)\right)^2 dx,\quad k=0,1,\cdots,r-1, \tag{3.1}$$

which is the sum of the normalized L^2 norm of the first $(r-1)$ derivatives of $\hat{f}^k(x)$.

In this section, we shall discuss the explicit and compact forms of β_k, which plays an important role in maintaining the symmetry of a symmetrical problem when solved by the high order $(2r-1>5)$ WENO schemes. For example, there are basically two forms of β_k available for the seventh and ninth order WENO scheme in the literature. They are the explicit form of β_k as given explicitly in Balsara et al. [5], Gerolymos et al. [10] and Arandiga et al. [2], and the compact form of β_k that can be found in the Appendix of the paper by Don et al. [9].

Remark 3.1. We note that Balsara et al. [3, 4] provide an alternative and equally effective compact expression for β_k by using the Legendre polynomials basis for the WENO reconstruction procedure as oppose to the polynomials basis [11], which is more commonly used in the literature. Readers who are interested in the former case are referred to [3] for details. Our preliminary study indicates that the results from either formulations are virtually identical. In this study, we will focus our discussion on the latter case.

3.1 The explicit form of the smoothness indicators β_k

In [2, 5, 10], the explicit long complex formulas of β_k for the seventh and higher order WENO scheme are given. For example, the β_0 for the ninth $(r=5, 2r-1=9)$ order WENO scheme is

$$\begin{aligned}\beta_0=&f_{j-4}(22658f_{j-4}-208501f_{j-3}+364863f_{j-2}-288007f_{j-1}+86329f_j)\\&+f_{j-3}(482963f_{j-3}-1704396f_{j-2}+1358458f_{j-1}-411487f_j)\\&+f_{j-2}(1521393f_{j-2}-2462076f_{j-1}+758823f_j)\\&+f_{j-1}(1020563f_{j-1}-649501f_j)+107918f_j.\end{aligned} \tag{3.2}$$

For the full set of β_k, see [5, 10] and others.

Due to the machine round-off floating points representation of a real number, these formulas with large coefficients are prone for rounding errors. This numerical error could lead to an undesirable erratic and chaotic behavior of a high order *nonlinear* WENO scheme for solving problems sensitive to small random perturbations. If the sensitive parameter ϵ is not sufficiently large (for example, $\epsilon=10^{-15}$), a negative small random β_k, for an even power parameter p, would reduce the effectiveness of ϵ and thus create

unnecessary random substencil bias in an under-resolved or discontinuous stencil, and for an odd power parameter p, might even destabilize the solution with negative weights once a while. Therefore, a significant loss of accuracy (at least 4-5 digits) can be expected for a high order WENO scheme.

3.2 The compact form of the smoothness indicators β_k

Alternatively, one can take advantage of the compact and relatively more numerical stable formula in computing the β_k according to [9]. Its basic description is reproduced here for the sake of completeness.

Given the $(2r-1)$ order WENO scheme, the k substencil S_k, and a set of functional value $f_n^k = f_{i+k-r+n}$, $n=1,\cdots,r$, defined on the global stencil S^{2r-1}, the $(r-1)\times(r-1)$ symmetric smoothness measuring matrix $\mathbf{C^r}$ and the $(r-1)\times r$ differentiation matrix $\mathbf{G^k}$, the smoothness indicators β_k based on (3.1) can be written compactly in a quadratic bilinear form

$$\beta_k = \left\langle \mathbf{v^k}, \mathbf{C^r v^k} \right\rangle, \tag{3.3}$$

where

$$\mathbf{v^k} = \mathbf{G^k f^k} \quad \text{with } f_n^k = f_{i+k-r+n}, \quad n=1,\cdots,r. \tag{3.4}$$

The matrices $\mathbf{G^k}$ up to the eleventh order WENO scheme can be found in [9].

For any given r, the elements of the symmetric smoothness measuring matrix $\mathbf{C^r}$ are

$$C^r_{m,n} = \sum_{\ell=1}^{\min\{m,n\}} \mathbf{A}^{\ell}_{m+\ell-1,n+\ell-1}. \tag{3.5}$$

(See [9] for the definition of $\mathbf{A}$). For example,

$$\mathbf{C^6} = \begin{bmatrix} 1 & 0 & 0 & 0 & 0 \\ 0 & \frac{13}{12} & 0 & -\frac{1}{720} & 0 \\ 0 & 0 & \frac{781}{720} & 0 & -\frac{43}{30240} \\ 0 & -\frac{1}{720} & 0 & \frac{32803}{30240} & 0 \\ 0 & 0 & -\frac{43}{30240} & 0 & \frac{1312121}{1209600} \end{bmatrix} = \mathbf{I} + \mathbf{H^6}, \tag{3.6}$$

where $\mathbf{I}$ is the identity matrix and

$$\mathbf{H^6} = \begin{bmatrix} 0 & 0 & 0 & 0 & 0 \\ 0 & \frac{1}{12} & 0 & -\frac{1}{720} & 0 \\ 0 & 0 & \frac{61}{720} & 0 & -\frac{43}{30240} \\ 0 & -\frac{1}{720} & 0 & \frac{2563}{30240} & 0 \\ 0 & 0 & -\frac{43}{30240} & 0 & \frac{102521}{1209600} \end{bmatrix}. \tag{3.7}$$

It should be noted that $\{\mathbf{C^k},\ k=1,\cdots,r-1\}$ are the leading principal minor of $\mathbf{C^r}$. For example, the smoothness measuring matrices $\{\mathbf{C^k},\ k=1,\cdots,5\}$ is a leading principal minor of $\mathbf{C^6}$. Hence, (3.1) or (3.3) can be rewritten as

$$\beta_k=\left\langle \mathbf{v^k},\mathbf{v^k}\right\rangle+\left\langle \mathbf{v^k},\mathbf{H^r v^k}\right\rangle=\mathbf{b}_k+\mathbf{h}_k, \tag{3.8}$$

where $\mathbf{b}_k=\left\langle \mathbf{v^k},\mathbf{v^k}\right\rangle$ contains only squared terms like $(v_i^k)^2$ with a unit coefficient while $\mathbf{h}_k$ contains all the remaining terms including all cross multiplied terms like $v_i^k v_j^k$, $i\neq j$.

For example, in the ninth $(r=5,\ 2r-1=9)$ order WENO scheme, we have

$$\beta_k=\sum_{l=1}^{4}(v_l^k)^2+\frac{61}{720}(v_3^k)^2+\frac{1}{12}(v_2^k)^2-\frac{1}{360}v_2^k v_4^k+\frac{2563}{30240}(v_4^k)^2, \tag{3.9}$$

with

$$\mathbf{b}_k=\sum_{l=1}^{4}(v_l^k)^2 \quad \text{and} \quad \mathbf{h}_k=\frac{61}{720}(v_3^k)^2+\frac{1}{12}(v_2^k)^2-\frac{1}{360}v_2^k v_4^k+\frac{2563}{30240}(v_4^k)^2.$$

In order to guarantee the positivity of β_k, one would need to replace all the cross multiplied terms and express all the terms related to the elements in the cross multiplied terms as sum of squares. In the following, we present three different approaches to achieve the above goal. The first one is to perform the brute force completion of squares iteratively with increasing complexity. The second one is the method of expansion which solves a small but increasingly complex system of equations iteratively. The last one is the method of Shur complement which solves a matrix equation via the mathematically elegant Shur complement method by taking advantage of the special structure of the matrix for any order of the WENO scheme. The first two approaches require that all the β_k of the WENO order $[1,3,\cdots,2r-3]$ are known before finding the β_k of the WENO order $2r-1$, thus they are less flexible. This is in contrast to the third approach that β_k of order $2r-1$ can be found for any given r.

3.2.1 Method of completion of squares

For example, the term $\frac{1}{360}v_2^k v_4^k$ in (3.9) should be eliminated from the equation by modifying the three terms involving v_2^k and v_4^k. This can be done by the simple technique of completing the square [†], and one obtains

$$\beta_k=\sum_{l=1}^{4}(v_l^k)^2+\frac{61}{720}(v_3^k)^2+\frac{1}{12}\left(v_2^k-\frac{1}{60}v_4^k\right)^2+\frac{949}{11200}(v_4^k)^2. \tag{3.10}$$

This simple procedure can be applied recursively for other cross multiplied terms for any high order WENO scheme.

[†] $ax^2-bxy+cy^2=a(x-\delta y)^2+\omega y^2$, where $ac\neq 0$, $\delta=b/(2a)$, $\omega=c-a\delta^2$.

3.2.2 Method of expansion

Instead, one can assume that the m-ary quadratic form has the sum of squares form (Here, we take the thirteen ($r=7$, $2r-1=13$, $m=(r-1)/2=3$) order WENO scheme for illustration)

$$\beta_k = a(x-by-cz)^2+d(y-ez)^2+fz^2, \tag{3.11}$$

where (a,b,c,d,e,f) are the ($2m=6$) unknown coefficients and, for clarity, we denote $x=v_2^k$, $y=v_4^k$, $z=v_6^k$. We shall determine the unknown coefficients by expanding (3.11) and matching the coefficients of the corresponding terms with the known values given in **F** (see (3.13) below). This results in a system of six equations with six unknown. After some straightforward algebraic manipulations, one can show that

$$\begin{pmatrix} a \\ b \\ c \\ d \\ e \\ f \end{pmatrix} = \begin{pmatrix} F_{11} \\ -F_{12}/a \\ -F_{13}/a \\ F_{22}-ab^2 \\ -(F_{23}-abc)/d \\ F_{33}-ac^2-de^2 \end{pmatrix} = \begin{pmatrix} \frac{1}{12} \\ \frac{1}{60} \\ -\frac{1}{2520} \\ \frac{949}{11200} \\ \frac{397}{23652} \\ \frac{559977250489}{6608785075200} \end{pmatrix}. \tag{3.12}$$

It is noteworthy that the coefficients (a,b,d) are exactly the same as the one given in the β_k of the ninth order ($r=5$) WENO scheme. Hence, there are actually only three unknowns coefficients (c,e,f) related to the new variable z are needed to be solved for. Similar pattern can be found in an even higher order β_k.

3.2.3 Method of Shur complement

One can also obtain the same results for the smoothness indicators β_k of arbitrary WENO order in a mathematically elegant way via the method of Shur complement (see [23] and reference therein). In general, since all the relevant terms involved in the cross multiplied terms in the β_k can be written compactly in a symmetric positive definite $m\times m$ (here, $m=\left[\frac{r-1}{2}\right]$) matrix **F** associated with a symmetric positive definite m-ary quadratic form with real coefficients (see below for example) as

$$\mathbf{F} = \begin{pmatrix} \mathbf{A} & \mathbf{B} \\ \mathbf{B}^{\mathrm{T}} & \mathbf{C} \end{pmatrix}, \tag{3.13}$$

where **A** is a $(m-1)\times(m-1)$ block symmetric matrix, **B** is a $(m-1)\times 1$ block matrix and **C** is a 1×1 block matrix.

Since **A** itself is a symmetric positive definite matrix and invertible, one can decompose the matrix **F** using the Shur complement of **A** in **F**, namely,

$$\begin{pmatrix} \mathbf{A} & \mathbf{B} \\ \mathbf{B}^{\mathrm{T}} & \mathbf{C} \end{pmatrix} = \begin{pmatrix} \mathbf{I} & \mathbf{B}^{\mathrm{T}}\mathbf{A}^{-1} \\ \mathbf{0} & \mathbf{I} \end{pmatrix}^{\mathrm{T}} \begin{pmatrix} \mathbf{A} & \mathbf{0} \\ \mathbf{0} & \mathbf{C}-\mathbf{B}^{\mathrm{T}}\mathbf{A}^{-1}\mathbf{B} \end{pmatrix} \begin{pmatrix} \mathbf{I} & \mathbf{B}^{\mathrm{T}}\mathbf{A}^{-1} \\ \mathbf{0} & \mathbf{I} \end{pmatrix} = \mathbf{L}^{\mathrm{T}}\mathbf{D}\mathbf{L},$$

where $\mathbf{D}=\mathrm{diag}(d_1,d_2,\cdots,d_{m-1},d_m)$ with d_i, $i=1,\cdots,m-1$ are the diagonal elements of **A** and $d_m=\mathbf{C}-\mathbf{B}^{\mathrm{T}}\mathbf{A}^{-1}\mathbf{B}$ with all $d_i>0$.

Recognizing that **A**, which is a symmetric positive definite matrix itself and associated with a symmetric positive definite $(m-1)$-ary quadratic form, can be decomposed, similarly to **F**, as $\mathbf{A}=\mathbf{L}^{\mathrm{T}}\mathbf{D}\mathbf{L}$, and $\mathbf{A}^{-1}$ can be readily found for an upper triangular block matrix by observing that

$$\begin{pmatrix} \mathbf{I} & \mathbf{B}^{\mathrm{T}}\mathbf{A}^{-1} \\ \mathbf{0} & \mathbf{I} \end{pmatrix}^{-1} = \begin{pmatrix} \mathbf{I} & -\mathbf{B}^{\mathrm{T}}\mathbf{A}^{-1} \\ \mathbf{0} & \mathbf{I} \end{pmatrix}. \tag{3.14}$$

Finally, by defining a new variable **u** in term of original variables involving the cross multiplied terms in β_k, **v**, such that $\mathbf{u}=\mathbf{v}\mathbf{L}^{\mathrm{T}}$, one can replace all the terms involving the elements in **v** with $\langle \mathbf{u},\mathbf{D}\mathbf{u}\rangle = d_1u_1^2+\cdots+d_mu_m^2$ in the formula of β_k.

For example, the cross multiplied term $\frac{1}{360}v_2^kv_4^k$ in (3.9) involves only the elements v_2^k and v_4^k, one can group and rewrite these three terms together as

$$\mathbf{v}^{\mathrm{T}}\mathbf{F}\mathbf{v}, \tag{3.15}$$

where

$$\mathbf{v}=\begin{pmatrix} v_2^k \\ v_4^k \end{pmatrix}, \quad \mathbf{F}=\begin{pmatrix} \frac{1}{12} & -\frac{1}{720} \\ -\frac{1}{720} & \frac{2563}{30240} \end{pmatrix}. \tag{3.16}$$

(Notice the relationship between the elements of **F** and $\mathbf{H}^{[5]}$).

Following the procedure above, one has

$$\mathbf{D}=(d_1,d_2)=\left(\frac{1}{12},\ \frac{949}{11200}\right), \quad \mathbf{u}=(u_1,u_2)=\left(v_2^k-\frac{1}{60}v_4^k,\ v_4^k\right), \tag{3.17}$$

and

$$\mathbf{h}_k=\frac{61}{720}(v_3^k)^2+d_1u_1^2+d_2u_2^2, \tag{3.18}$$

which is exactly what we have obtained earlier.

In Appendix A, a symbolic Matlab code is provided to illustrate the application of the method of Shur complement that performs the sum of perfect squares for the thirteen order WENO scheme. Extension to higher order WENO scheme can be easily derived following the same procedure.

3.3 Unified compact form of the smoothness indicators β_k

In fact, one can express the compact form of β_k of any order in a mathematically elegant way as (For simplicity, we illustrate the concept with order $(2r-1, 2\leq r\leq 7)$)

$$\beta_k=\left\langle \mathbf{v^k},\mathbf{v^k}\right\rangle+\mathbf{a}_e\mathbf{B}_e^2+\mathbf{a}_o\mathbf{B}_o^2, \tag{3.19}$$

where $\mathbf{v^k}=\mathbf{G^k f^k}=\left(v_1^k,v_2^k,\cdots,v_{r-1}^k\right)$ with $f_n^k=f_{i+k-r+n}$, $n=1,\cdots,r$,

$$\mathbf{a}_e=\begin{bmatrix} a_2 & a_4 & a_6 \end{bmatrix},\quad \mathbf{a}_o=\begin{bmatrix} a_3 & a_5 & a_7 \end{bmatrix}, \tag{3.20}$$

and

$$\mathbf{B}_e=\begin{bmatrix} 1 & -b_4 & -c_6\\ 0 & 1 & -b_6\\ 0 & 0 & 1 \end{bmatrix}\begin{bmatrix} v_2^k\\ v_4^k\\ v_6^k \end{bmatrix},\quad \mathbf{B}_o=\begin{bmatrix} 1 & -b_5 & -c_7\\ 0 & 1 & -b_7\\ 0 & 0 & 1 \end{bmatrix}\begin{bmatrix} v_3^k\\ v_5^k\\ v_7^k \end{bmatrix}, \tag{3.21}$$

or, explicitly as

$$\begin{aligned}\beta_k=&\sum_{l=1}^{r-1}(v_l^k)^2+a_2\left(v_2^k-b_4v_4^k-c_6v_6^k\right)^2+a_4\left(v_4^k-b_6v_6^k\right)^2+a_6\left(v_6^k\right)^2\\&+a_3\left(v_3^k-b_5v_5^k-c_7v_7^k\right)^2+a_5\left(v_5^k-b_7v_7^k\right)^2+a_7\left(v_7^k\right)^2.\end{aligned} \tag{3.22}$$

The coefficients (a_m,b_m,c_m), $m=2,\cdots,r$ are given in the Table 1. The β_k of any $(2r-1,$ $2\leq r\leq 7)$ order can be obtained by setting the corresponding coefficients $(a_m=0,\ b_m=0,$ $c_m=0)$, $m\geq r-1$. Extension to order greater than thirteen $(r>7)$ is trivial in either one of these two unified compact forms once the coefficients are found via one of the methods above.

Remark 3.2. We remark that the coefficients appeared in the compact form of β_k are $\mathcal{O}(1)$ and are generally only slightly larger than one despite the size of the numerator and denominator. Hence, the compact form of β_k has a better numerical stability than the explicit form.

Furthermore, regarding the implementation of these coefficients in an algorithm, the numerical value of these coefficients can be computed with extra precision or symbolically and stored with extra precision as data in the program.

Table 1: The coefficients (a_m,b_m,c_m), $m=2,\cdots,7$ of the unified compact form of the smoothness indicators β_k.

$a_2=\frac{1}{12}$	$b_4=\frac{1}{60}$	$c_6=-\frac{1}{2520}$
$a_3=\frac{61}{720}$	$b_5=\frac{43}{2562}$	$c_7=0$
$a_4=\frac{949}{11200}$	$b_6=\frac{397}{23652}$	
$a_5=\frac{131292421}{1549497600}$	$b_7=0$	
$a_6=\frac{559977250489}{6608785075200}$		
$a_7=0$		

4 Numerical results and discussion

In this section, we present the symmetry property of symmetrical problems computed by the high order WENO schemes. The influence of the β_k for the symmetry problems will be shown. We shall refer to the WENO scheme (JS/Z) with the explicit form of β_k given by Balsara et al. [5] as the WENO-JS/Z-BS, and the compact form of β_k given by Don et al. [9] as the WENO-JS/Z-DB in the following discussions.

Since we are interested in the examining the symmetry property of the high order WENO scheme, we shall examine the temporal evolution of the error in term of the loss of symmetry along a direction where the solution is supposedly symmetrical. We shall give the definition that quantify the global l_2 symmetry error $E_s(f,t)$ as follow

Definition 4.1. Given a function $f(x,y,t)$, assuming symmetric along the x-direction in a domain $x\in[0,L],y\in[0,H]$, the symmetry error $E_s(f,t)$ of f is defined as

$$E_s(f,t)=\left(\frac{1}{2NM}\sum_{i,j}\big(f(x_i,y_j,t)-f(L-x_i,y_j,t)\big)^2\right)^{\frac{1}{2}}, \tag{4.1}$$

where $x_i=iL/N$, $i=0,\cdots,N$ and $y_j=jH/M$, $j=0,\cdots,M$.

In the characteristic-wise WENO finite difference scheme that used in this study, the polynomial reconstruction procedure is applied to the characteristic projection (via Roe eigensystem) of the positive and negative fluxes after applying the global Lax-Friedrichs flux splitting of the Euler flux above [11]. The resulting system of ODEs after the spatial discretization is advanced in time via the third order TVD Runge-Kutta scheme [20]. Unless stated otherwise, the CFL condition is set to be CFL$=0.45$, and the sensitivity and power parameter in the WENO nonlinear weights are set to be $\epsilon=1\times10^{-12}$ and $p=2$ respectively, in the numerical experiments performed in this study.

4.1 One-dimensional problems

The one-dimensional double rarefaction problem and Sedov blast wave problem are investigated to demonstrate the behaviors of the WENO-JS/Z-BS and WENO-JS/Z-DB schemes for the symmetrical problems in this section.

4.1.1 Double rarefaction problem

The initial conditions of the double rarefaction problem are

$$(\rho,u,P)=\begin{cases}(1,-2,0.4), & -5\le x<0,\\ (1,2,0.4), & 0\le x\le 5,\end{cases}$$

and the final time is $t=1$. The number of uniform cells used is $N=200$.

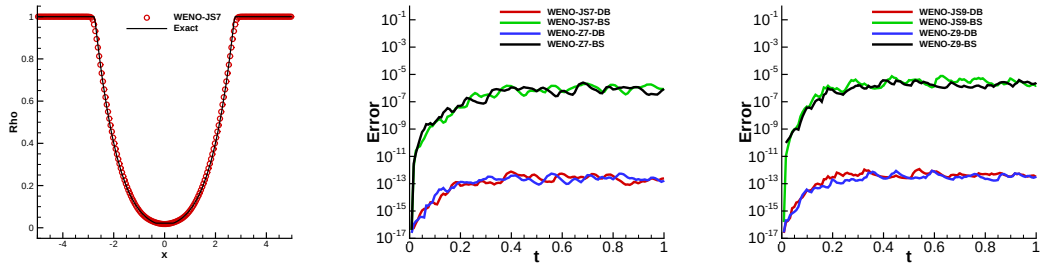

(a) Density (b) $E_s(\rho,t)$, WENO-7 (c) $E_s(\rho,t)$, WENO-9

Figure 2: One-dimensional double rarefaction problem. (a) The density profile computed by the WENO-JS7 scheme at time $t=1$ and the symmetry errors of the density computed by (b) the WENO-JS/Z7 and (c) the WENO-JS/Z9 schemes.

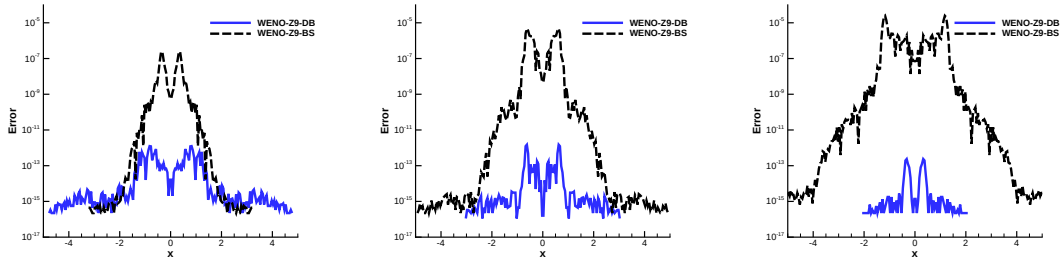

(a) $t=0.1$ (b) $t=0.2$ (c) $t=0.4$

Figure 3: One-dimensional double rarefaction problem. The temporal evolution of the symmetry errors of the density computed by the WENO-Z9 scheme at times (a) $t=0.1$, (b) $t=0.2$ and (c) $t=0.4$.

In the left figure of Fig. 2, the density profile computed by the WENO-JS7 scheme and the exact solution are shown. Similar results computed by the WENO-Z7 and WENO-JS/Z9 are omitted here for clarity. The symmetry errors of the density computed by seventh and ninth order WENO-JS7/9 and WENO-Z7/9 schemes are shown in the middle and right figures of Fig. 2 respectively. It can be observed that the symmetry errors with the compact form of β_k (3.3) are at least six digits smaller than those computed with the explicit form of β_k (3.2).

For the purpose of clarity, we show the temporal evolution of the symmetry error computed by the WENO-Z9 scheme in space at times $t=0.1$, $t=0.2$ and $t=0.4$ in Fig. 3. From the temporal-spatial solution of the density, the largest symmetry error is located at the corner of the rarefaction wave (a jump in the derivative of the density) and the constant left/right states. The results show that, with the explicit form of β_k, the symmetry error increases rapidly to a large value of $\mathcal{O}(10^{-7})$ in the early time and then grows slowly up to a value of $\mathcal{O}(10^{-5})$ afterward. By comparison, with the compact form of β_k, the symmetry error also grows rapidly at the early time but at a much lesser rate to

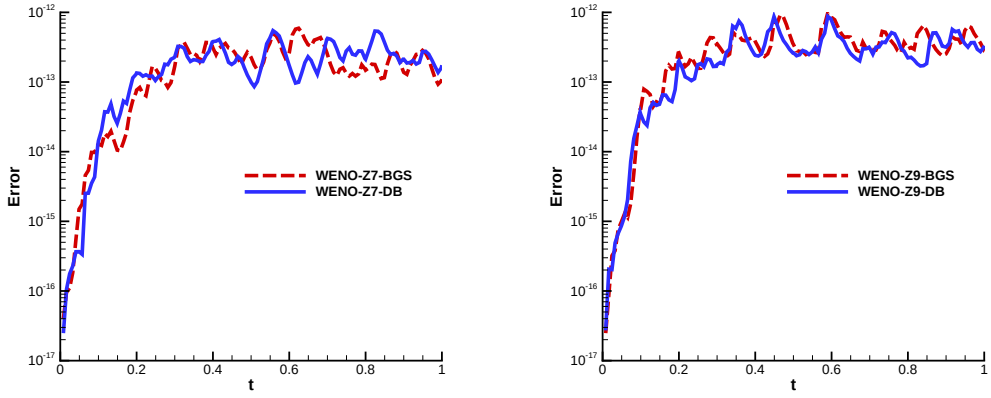

(a) (b)

Figure 4: One-dimensional double rarefaction problem. The symmetry errors of the density computed by the (a) WENO-Z7 and (b) WENO-Z9 scheme at time $t=1$ with compact form of β_k (blue solid line: present study, and red dashed line: [3]).

a value of $\mathcal{O}(10^{-13})$ and then grows slowly and remains more or less around a value of $\mathcal{O}(10^{-12})$ afterward.

Furthermore, we show the comparative results with the present compact form and the compact form of β_k given in [3, 4] in Fig. 4, which demonstrates no discernible difference between the two compact forms of β_k. In essence, user can choose either version of compact form of β_k as convenient in term of reducing the symmetry error, and the numerical results studied here hold for both forms.

One might ask what role does the sensitivity parameter ϵ plays in term of the symmetry error in light of two different forms of β_k. In this regard, we show two figures (Fig. 5) which indicate the effect of the ϵ on the symmetry error of the one-dimensional double rarefaction problem. They clearly show that, for any fixed ϵ, the compact form of β_k out-performs the explicit form of β_k for a wide range of ϵ. Furthermore, for large ϵ, the β_k is effectively unimportant relative to ϵ. Hence, as expected, the symmetry error will be reduced. As the in-depth study in [12], for essentially *non-oscillatory* shock capturing, it is important to keep ϵ small, say 10^{-12}. As the matter of fact, ϵ should be a zero or machine zero in an ideal situation for effective shock capturing.

4.1.2 Sedov blast-wave problem

The Sedov blast-wave problem [18,24] is a shocked flow with a large pressure ratio and a very low pressure. A high pressure point-blast wave propagates into a very low pressure region. The initial conditions are

$$(\rho,u,P)=\begin{cases}(1,0,4\times10^{-13}), & \delta<|x|<2,\\ (1,0,2.56\times10^{8}), & |x|<\delta,\end{cases}\qquad \delta=\frac{\Delta x}{2}, \tag{4.2}$$

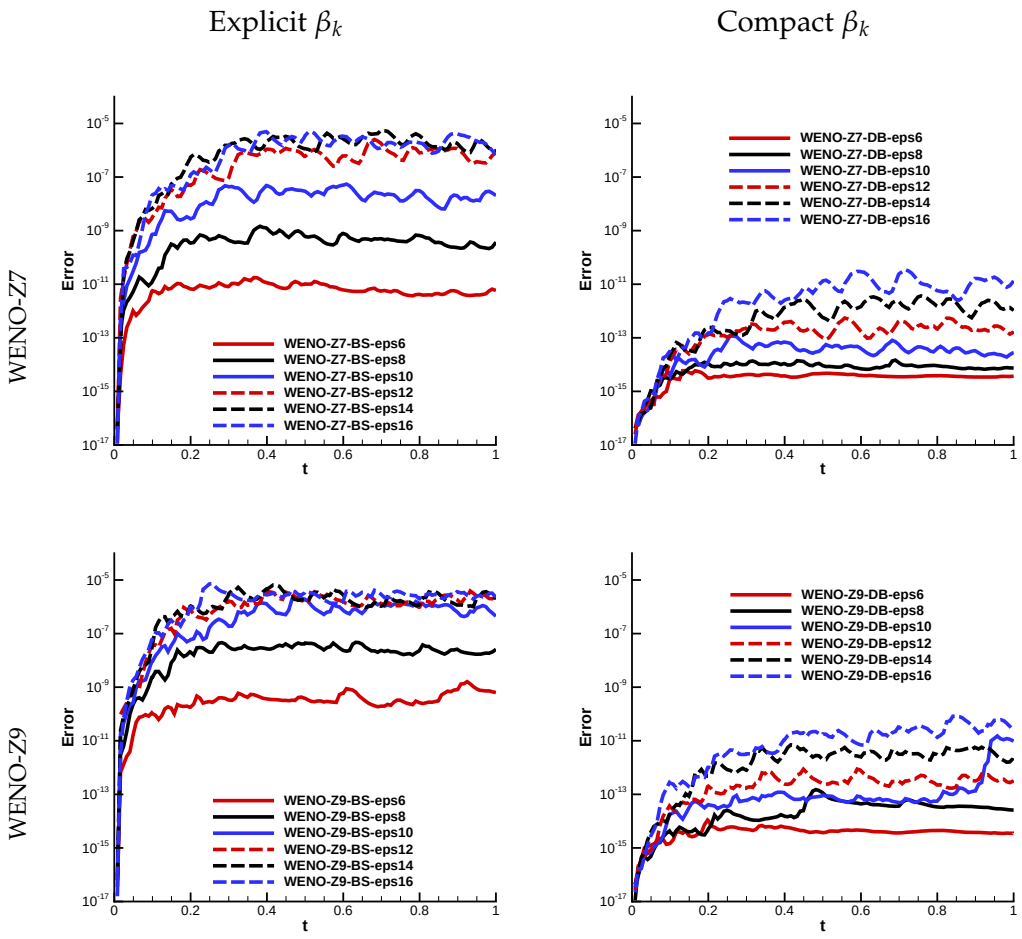

Figure 5: One-dimensional double rarefaction problem. The symmetry errors of the density computed by the WENO-Z7 and WENO-Z9 schemes with different ϵ (eps$*=10^{-*}$) at time $t=1$ (Left) the explicit and (Right) compact form of β_k.

with $\gamma=1.4$, $\Delta x=5\times10^{-3}$ and final time $t=10^{-3}$. The number of uniform cells used is $N=800$.

In the left figure of Fig. 6, the density profile computed by the WENO-JS7 scheme and the exact solution are shown. Similar results computed by the WENO-Z7 and WENO-JS/Z9 are omitted here for clarity. The symmetry errors of the density computed by the seventh and ninth order WENO-JS7/9 and WENO-Z7/9 schemes are shown in the middle and right figures of Fig. 2 respectively. It can be observed that the symmetry errors with the compact form of β_k (3.3) are at least five digits smaller than those computed with the explicit form of β_k (3.2). In this case, however, the symmetry error of the WENO-Z9-DB scheme is only two to three digits smaller than that of the WENO-JS9-BS scheme. We have not found out the reason for this behavior for the ninth order WENO-Z9 scheme

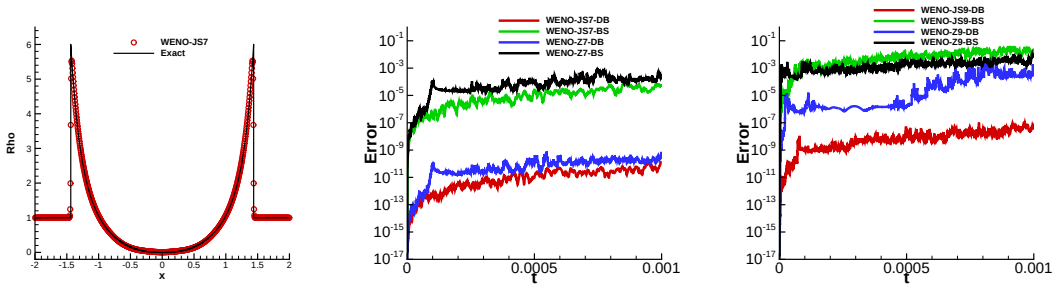

(a) Density (b) $E_s(\rho,t)$, WENO-7 (c) $E_s(\rho,t)$, WENO-9

Figure 6: One-dimensional Sedov blast-wave problem. (a) The density profile computed by the WENO-JS7 scheme at time $t=10^{-3}$ and the symmetry errors of the density computed by (b) the WENO-JS/Z7 and (c) the WENO-JS/Z9 schemes.

yet and will report it in the future work if any improvement can be made. Nonetheless, these two simple examples have clearly demonstrated that the rapid loss of symmetry is related to the explicit form of β_k in the high order WENO scheme.

4.2 Two-dimensional Rayleigh-Taylor instability problem

In this section, we consider the two-dimensional Rayleigh-Taylor instability (RTI) problem for investigating the Symmetry property of the high order WENO schemes. The problem is set up as follows: the computational domain is $[0,\frac{1}{4}]\times[0,1]$ with a perturbed interface located at $y=\frac{1}{2}$ initially. The heavy fluid with density $\rho=2$ is below the interface, and the light fluid with density $\rho=1$ is above the interface with the acceleration in the positive y-direction. The pressure P is continuous across the interface and a small perturbation is given to the y-direction fluid speed. That is, for $0\le y<\frac{1}{2}$, we have $\rho=2$, $u=0$, $p=2y+1$, $v=v_0\cos(2\pi kx)$, and for $\frac{1}{2}\le y\le 1$, $\rho=1$, $u=0$, $p=y+\frac{3}{2}$, $v=-v_0\cos(2\pi kx)$, where $k=4$, $v_0=-0.025c$, $c=\sqrt{\gamma P/\rho}$ is the sound speed, and the ratio of specific heats $\gamma=\frac{5}{3}$. The reflective boundary conditions are imposed on the left and right boundaries. At the top boundary, the flow values are set as $\rho=1$, $p=2.5$, $u=v=0$, and at the bottom boundary, they are $\rho=2$, $p=1$, $u=v=0$. The source terms ρ is added to the right hand side of third equation, and ρv is added to the fourth equation of Euler equations. The final simulation time is $t=1.95$.

In Figs. 7 and 8, we show the contour lines of the density computed by the classical WENO-JS7 and WENO-JS9 schemes under different mesh resolutions. From the figures, it is very difficult to identify the difference among the figures computed by the WENO-JS7/9 with two different forms of β_k under the resolutions $\Delta x=1/480,1/960$. In the case of the highest resolution $\Delta x=1/1920$, the WENO-JS7-BS scheme generates a slightly asymmetric figure (e.g., structures in the red boxes) but the WENO-JS7-DB scheme preserves the symmetry of the result. Furthermore, there are some minor different structures observed in the results computed by the WENO-JS9-BS and WENO-JS9-DB schemes. The

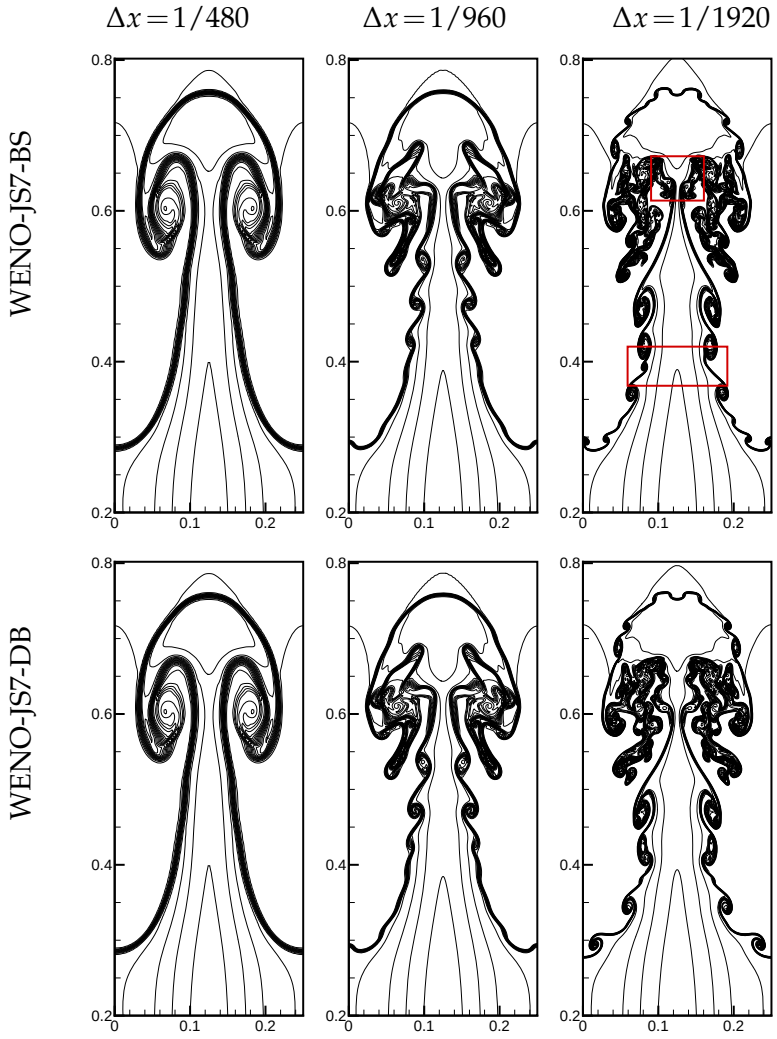

Figure 7: Two-dimensional Rayleigh-Taylors instability. The density $\rho(x,y,t=1.95)$ computed by the WENO-JS7-BS and WENO-JS7-DB schemes.

corresponding symmetry errors of density are plotted in Fig. 9. We can easily find that the symmetry errors computed by the WENO-JS7/9 schemes with the compact form of β_k (3.3) are around 3-4 digits smaller than those with the explicit form of β_k (3.2) under different resolutions.

5 Conclusion remarks

The symmetry property of the nonlinear seventh and ninth order characteristic-wise weighted essentially non-oscillatory (WENO) finite difference shock capturing scheme

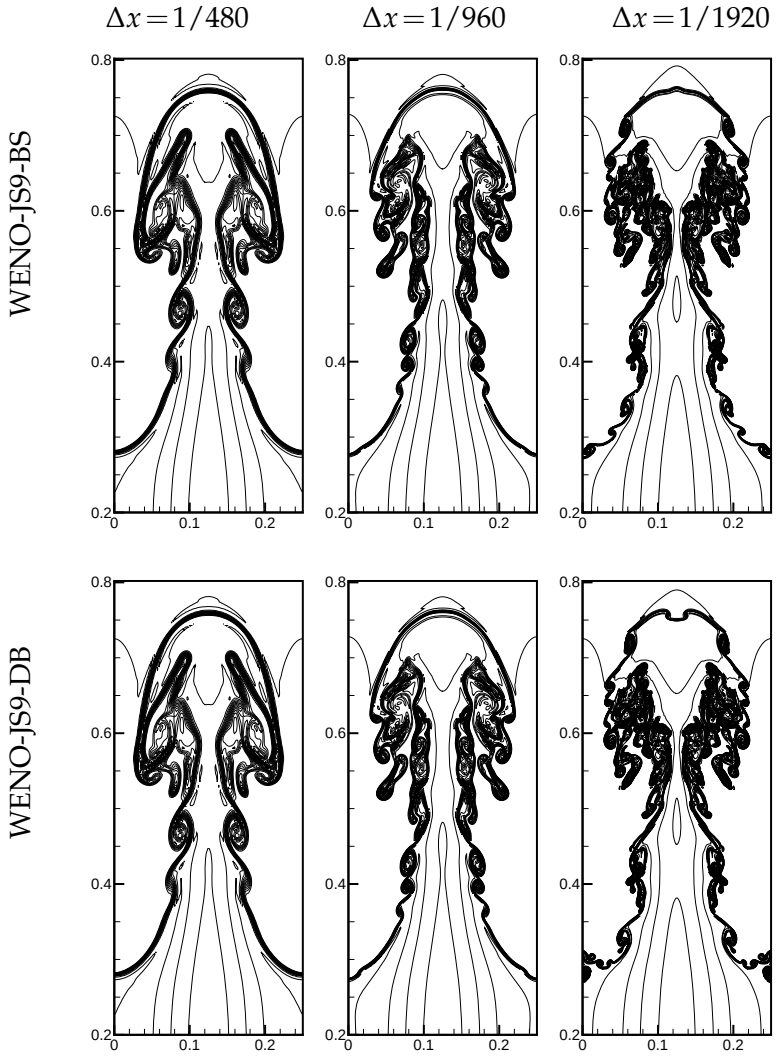

Figure 8: Two-dimensional Rayleigh-Taylors instability. The density $\rho(x,y,t=1.95)$ computed by the WENO-JS9-BS and WENO-JS9-DB schemes.

with the global Lax-Friedrichs flux splitting via the Roe-averaged eigensystem was investigated in this study. We found that the explicit and compact forms of β_k in the nonlinear weights definition of the WENO scheme play an important role in the rapid loss of symmetry property in the solution. The explicit form of β_k is prone for rounding errors because of the large coefficients. Therefore, an alternative compact and stable formula in computing high order β_k is derived and strongly recommended for simulations employing a high order WENO scheme. The numerical results of the one-dimensional double rarefaction and Sedov blast-wave problems, and the two-dimensional Rayleigh-Taylor instability problem demonstrated that the symmetry errors computed by the high order

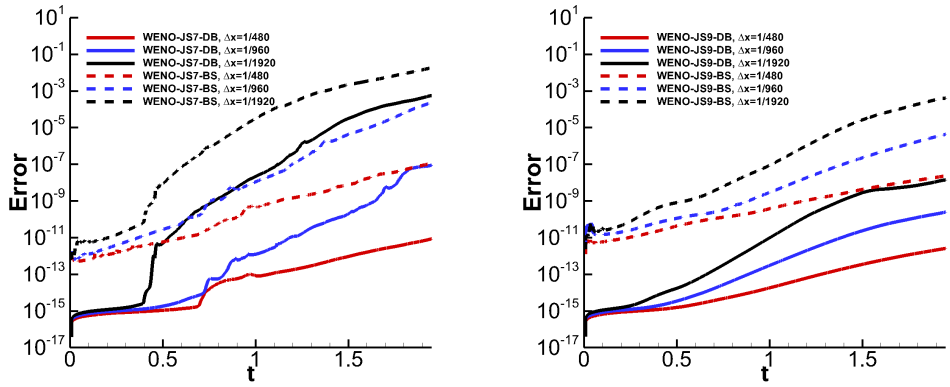

(a) $E_s(\rho,t)$, WENO-JS7 (b) $E_s(\rho,t)$, WENO-JS9

Figure 9: Two-dimensional Rayleigh-Taylors instability. The symmetry error of density computed by (a) the WENO-JS7 and (b) the WENO-JS9 schemes.

WENO scheme with the compact form of β_k can be substantially smaller than those with the explicit one. Even though the benefits of using the compact form of β_k is illustrated with problems with symmetrical solutions, the numerical solutions of non-symmetrical strongly non-linear problems can also be benefited in terms of improved numerical stability, reduced rounding errors and increased computational efficiency.

Appendix

A Matlab code for sum of squares via Shur complement

```
clear all;

F = sym('f', 3);
F(1,1) =         13/sym(        12)  ;
F(1,2) =         -1/sym(       720)  ; F(2,1) = F(1,2) ;
F(2,2) =      32803/sym(     30240)  ;
F(1,3) =          1/sym(     30240)  ; F(3,1) = F(1,3) ;
F(2,3) =      -1721/sym(   1209600)  ; F(3,2) = F(2,3) ;
F(3,3) = 259799963/sym(239500800)  ;

F = F-eye(3)

%----------------------------------------
A = sym('a',1); B = sym('b',[1 1]) ; C = sym('c',1); d = sym('d',2);
A = F(1,1)
```

```
B = F(1,2)
C = F(2,2)

d  = diag( [ A, sym(C - B'*inv(A)*B) ] )
L0 = sym(eye(2)); L0(1,2)     = sym(B'*inv(A))

L  = L0

G = L'*d*L

V = sym('v',[1,2]);
U = transpose(V*L')

%-----------------------------------------------------------
L2 = sym(eye(3)); L2(1:2,1:2) = L
%-----------------------------------------------------------
A = sym('a',2); B = sym('b',[2 1]) ; C = sym('c',1); D = sym('d',3);
A = F(1:2,1:2)
B = F(1:2,3)
C = F(3,3)

D  = diag( [ diag(d)', sym(C - B'*inv(A)*B) ])
L3 = sym(eye(3)); L3(1:2,3) = sym(B'*inv(A))

L = L2*L3

G = L'*D*L

V = sym('v',[1,3]);
U = transpose(V*L')
D
Y = sum(diag(D).*(U.^2))
```

Acknowledgements

The authors would like to acknowledge the funding support of this research by the National Natural Science Foundation of China (Nos. 11801383, 11871443), National Science and Technology Major Project (No. 20101010), Shandong Provincial Natural Science Foundation (No. ZR2017MA016) and Fundamental Research Funds for the Central Universities (No. 201562012). The authors (Li and Don) also like to thank Shijiazhuang Tiedao University and Ocean University of China for providing the startup

funds (No. Z6811021064 and 201712011), respectively.

References

[1] N. N. Anuchina, V. I. Volkov, V. A. Gordeychuk, N. S. Es'kov, O. S. Ilyutina and O. M. Kozyrev, *Numerical simulations of Rayleigh-Taylor and Richtmyer-Meshkov instability using MAH-3 code*, J. Comput. Appl. Math., 168 (2004), pp. 11–20.
[2] F. Arándiga, A. Baeza, A. M. Belda and P. Mulet, *Analysis of WENO schemes for full and global accuracy*, SIAM J. Numer. Anal., 49 (2011), pp. 893–915.
[3] D. S. Balsara, S. Garain and C.-W. Shu, *An efficient class of WENO schemes with adaptive order*, J. Comp. Phys., 326 (2016), pp. 780–804.
[4] D. S. Balsara, T. Rumpf, M. Dumbser and C.-D. Munz, *Efficient, high accuracy ADER-WENO schemes for hydrodynamics and divergence-free magnetohydrodynamics*, J. Comp. Phys., 228 (2009), pp. 2480–2516.
[5] D. S. Balsara and C.-W. Shu, *Monotonicity preserving weighted essentially non-oscillatory schemes with increasingly high order of accuracy*, J. Comput. Phys., 160 (2000), pp. 405–452.
[6] R. Borges, M. Carmona, B. Costa and W. S. Don, *An improved weighted essentially non-oscillatory scheme for hyperbolic conservation laws*, J. Comput. Phys., 227 (2008), pp. 3101–3211.
[7] M. Brouillette, *The Richtmyer-Meshkov instability*, Annu. Rev. Fluid Mech., 34 (2002), pp. 445–468.
[8] M. Castro, B. Costa and W. S. Don, *High order weighted essentially non-oscillatory WENO-Z schemes for hyperbolic conservation laws*, J. Comput. Phys., 230 (2011), pp. 1766–1792.
[9] W. S. Don and R. Borges, *Accuracy of the weighted essentially non-oscillatory conservative finite difference schemes*, J. Comput. Phys., 250 (2013), pp. 347–372.
[10] G. A. Gerolymos, D. Sénéchal and I. Vallet, *Very-high-order WENO schemes*, J. Comput. Phys., 228(23) (2009), pp. 8481–8524.
[11] G. S. Jiang and C.-W. Shu, *Efficient implementation of weighted ENO schemes*, J. Comput. Phys., 126 (1996), pp. 202–228.
[12] F. L. Jia, Z. Gao and W.-S. Don, *A spectral study on the dissipation and dispersion of the WENO schemes* , J. Sci. Comput., 63 (2015), pp. 49–77.
[13] V. P. Korobeinikov, Problems of Point-Blast Theroy, American Institute of Physics, (1991).
[14] M. Latini, O. Schilling, and W. S. Don, *Effects of order of WENO flux reconstruction and spatial resolution on reshocked two-dimensional Richtmyer-Meshkov instability*, J. Comput. Phys., 221 (2007), pp. 805–836.
[15] D. Lecoanet, I. J. Parrish and E. Quataert, *The dynamics of Rayleigh-Taylor stable and unstable contact discontinuities with anisotropic thermal conduction*, Mon. Not. R. Astron. Soc., 423 (2012), pp. 1866–1882.
[16] G. Li, C. Lu and J. Qiu, *Hybrid well-balanced WENO schemes with different indicators for shallow water equations*, Adv. Comput. Math., 40 (2014), pp. 747–772.
[17] O. Schilling, M. Latini, and W. S. Don, *Physics of reshock and mixing in single-mode Richtmyer-Meshkov instability*, Phys. Rev. E, 76 (2007), 026319.
[18] L. I. Sedov, Similarity and Dimensional Methods in Mechanics, Academic Press, New York, 1959.
[19] C.-W. Shu, *High order weighted essentially non-oscillatory schemes for convection dominated problems*, SIAM Rev., 51 (2009), pp. 82–126.

[20] C.-W. SHU AND S. OSHER, *Efficient implementation of essentially non-oscillatory shock-capturing schemes*, J. Comput. Phys., 77 (1988), pp. 439–471.
[21] V. K. TRITSCHLER, M. ZUBEL, S. HICKEL AND N. A. ADAMS, *Evolution of length scales and statistics of Richtmyer-Meshkov instability from direct numerical simulations*, Phys. Rev. E, 90 (2014), 063001.
[22] G. TRYGGVASON, *Numerical simulations of the Rayleigh-Taylor instability*, J. Comput. Phys., 75(2) (1988), pp. 253–282.
[23] F. ZHANG, The Schur Complement and Its Applications, Springer, doi:10.1007/b105056, Online ISBN 978-0-387-24273-6, 2005.
[24] X. X. ZHANG AND C.-W. SHU, *Positivity-preserving high order finite difference WENO schemes for compressible Euler equations*, J. Comput. Phys., 231 (2012), pp. 2245–2258.
[25] Y. T. ZHANG, C.-W. SHU AND Y. ZHOU, *Effects of shock waves on Rayleigh-Taylor instability*, Phys. Plasmas, 13 (2006), 062705.